

Improved Coverage in Dynamic Contrast-Enhanced Cardiac MRI Using Interleaved Gradient-Echo EPI

Shujun Ding, Steven D. Wolff, Frederick H. Epstein

An interleaved gradient-echo echo-planar imaging (IGEPI) sequence was modified for and applied to dynamic contrast-enhanced imaging of the heart. Using IGEPI, images with 3.0×3.9 mm nominal in-plane resolution are acquired in 100 ms, enabling eight slices per heartbeat for a heart rate of 60 beats/min. The acquisition speed and use of saturation prepulses allows acquisition of short- and long-axis images during the same contrast bolus. IGEPI maintains the acquisition characteristics required for performing a quantitative first-pass perfusion analysis as well as providing improved coverage compared with conventional fast gradient echo.

Key words: myocardium; perfusion; first-pass; contrast enhancement.

INTRODUCTION

Radionuclide scintigraphy with thallium-201- or technetium-99m-labeled perfusion agents is the most widely available and commonly used clinical method for the assessment of regional myocardial perfusion deficits (1). However, this technique is limited by attenuation artifacts from soft tissue and relatively poor spatial resolution, especially since the data acquisition occurs over many respiratory cycles. Positron emission tomography with ^{13}N -labeled ammonia (2, 3) or ^{15}O -labeled water (4) is considered a more accurate test; however, it is expensive and not widely available. Both tests use ionizing radiation. Magnetic resonance imaging is widely available and has the potential of producing perfusion images at higher resolution than nuclear medicine techniques (5, 6).

First-pass contrast-enhanced MRI of the heart has been used in many studies to assess cardiac perfusion. Some studies have been semiquantitative (7–10). Other studies have attempted to be truly quantitative with regard to assessing blood flow in ml/min per gram of tissue (11). The latter case requires that as well as imaging the uptake of contrast agent within the myocardium, the input function (i.e., the indicator flowing into the myocardial vasculature) be estimated.

The ideal acquisition requirements for a first-pass contrast-enhanced perfusion measurement of the heart in-

clude: (a) coverage of the entire heart; (b) adequate temporal resolution; (c) adequate image quality (signal-to-noise ratio, artifacts, *etc.*); (d) measurement of the input function (for quantitation); and (e) a linear, or at least quantifiable, relationship between signal intensity and contrast agent concentration (for quantitation) (12). Acquisition methods that approach these goals have included fast gradient-echo (10, 13, 14) and single- and dual-shot echo-planar imaging (EPI) (15–17).

Fast gradient echo (or turbo fast low angle shot (turbo-FLASH)) has been used in quantitative perfusion studies because it satisfies most of the requirements listed above (11). The major drawback of fast gradient echo is that it affords limited coverage of the heart. Specifically, with fast gradient echo, single short-axis images have been acquired in 160 to 590 ms, which means that for a heart rate of 60 beats/min, only one to five slices can be acquired per injection (10, 13, 18). Single- and dual-shot EPI can acquire images quickly enough to cover the entire heart during the first pass of a contrast bolus (15–17). However, these techniques are prone to geometric and intensity distortions due to susceptibility interfaces around the heart (19). Furthermore, single- and dual-shot EPI have been presented in spin-echo mode where blood in the ventricular cavity appears dark (i.e., the input function is not measured), making it incompatible for quantitative perfusion analysis.

An interleaved gradient-echo EPI (IGEPI) sequence that uses a short repetition time (TR) and a relatively short echo train per TR could provide better coverage of the heart than fast gradient echo, be less sensitive to susceptibility-related artifacts than single- or dual-shot EPI (20–22), and could maintain the ability to measure the input function and have a linear relationship between signal intensity and contrast agent concentration. Interleaved EPI was previously described by Cho *et al.* (20) and Farzaneh *et al.* (21). McKinnon (22) extended the idea and applied IGEPI to cardiac imaging but did not tailor it for or apply it to imaging the heart after a contrast agent injection. Fischer *et al.* (23, 24) have shown promising initial results using IGEPI for dynamic contrast-enhanced cardiac imaging, but they only acquired three slices per heartbeat on a single imaging axis using their approach. In this communication, we describe modifications to IGEPI for first-pass contrast-enhanced imaging of the heart, develop a set of imaging parameters that achieves improved coverage compared to fast gradient echo, show example images which demonstrate the resulting coverage and image quality, and demonstrate that this technique is similar to fast gradient echo regarding image acquisition requirements for quantitative perfusion analysis.

MRM 39:514–519 (1998)

From the Laboratory of Cardiac Energetics, National Heart, Lung, and Blood Institute (S.D., S.D.W.), National Institutes of Health, Bethesda, Maryland and Applied Science Laboratory, General Electric Medical Systems (F.H.E.), Waukesha, Wisconsin.

Address correspondence to: Shujun Ding, Ph.D., National Institutes of Health, 10 Center Drive - MSC 1061, Building #10, Room B1D161, Bethesda, MD 20892-1061.

Received August 25, 1997; revised November 21, 1997; accepted November 21, 1997.

0740-3194/98 \$3.00

Copyright © 1998 by Williams & Wilkins

All rights of reproduction in any form reserved.

MATERIALS AND METHODS

IGEPI was implemented previously by a few groups (20–22). The following modifications were made for contrast-enhanced first-pass cardiac imaging. To obtain T_1 weighting and to minimize the effect of R-R interval variation, a volumetric 90° saturation pulse is applied before the acquisition of each slice (14, 18), as shown in Fig. 1a. The saturation pulse is followed by a gradient crusher pulse to dephase the transverse magnetization.

Also, a modified centric phase encoding scheme was used (Fig. 1b). Like centric phase encoding, the central k -space lines are acquired with the first echo to minimize the effective TE (TE_{eff}) and susceptibility effects. However, unlike conventional centric phase encoding, the central k -space lines are ordered sequentially. This increases the effective delay between the saturation pulse and the most central k -space lines while still providing a smooth transition across the center of k_y -space to minimize image artifacts. A phase rewinding gradient is applied at the end of each TR.

Imaging was performed on a 1.5-T Horizon EchoSpeed Scanner (General Electric Medical Systems, Milwaukee, WI) equipped with enhanced gradient and receiver subsystems. For this study, the maximum gradient slew rate was limited to 120 mT/m/ms. The maximum gradient amplitude was 34 mT/m. A four-element phased-array RF coil (General Electric Medical Systems, Milwaukee, WI) was used for reception. The maximum receiver bandwidth was ± 200 kHz.

Imaging parameters were as follows: slice thickness, 8 mm; field of view, 36–39 cm; echo train length (ETL), 4; acquisition matrix, 128×48 –72; flip angle, 10° ; TR, 6.6 to 7 ms; TE_{eff} , 2.0 ms (calculated as the TE for the first echo that comprises the central lines); delay after saturation pulse, 20 ms; and receiver bandwidth, ± 125 KHz. Flow compensation (first-order gradient moment nulling) in the slice-select and read-out directions was ap-

plied for the first echo. These parameters achieve 1.65 to 1.75 ms/ k_y line in the k -space, or approximately 80 to 126 ms (or 12–18 TRs) for 48 to 72 k_y lines. Including the length of the saturation pulse and the delay before image acquisition, each image is acquired in 100 to 146 ms.

All studies of normal volunteers were conducted with the approval of the Institutional Review Board of National Heart, Lung, and Blood Institute. Written, informed consent was obtained from each subject before the MR examination. The average resting heart rate ranged from 56 to 67 beats/min. For the first-pass perfusion studies, gadopentetate dimeglumine (Magnevist, Berlex Laboratories, Wayne, NJ) was injected as a bolus into an antecubital vein (dose, 0.04–0.07 mmol/kg; rate, 3 ml/s). This was immediately followed by a bolus of normal saline (dose, 15 ml; rate, 3 ml/s). An MR-compatible power injector (Medrad, Inc., Pittsburgh, PA) was used for all injections.

Image acquisition began with contrast administration. Six to eight double-oblique images were acquired depending on the subject's heart rate and the precise acquisition parameters. Images were continuously acquired for 30 to 40 s. Subjects were instructed to breath-hold at the start of image acquisition and to maintain the breath-hold for as long as was comfortable. In each case, the breath-hold time exceeded the time for the contrast bolus to wash through the myocardium in the first pass (<30 s).

Signal intensity levels were determined over time in regions of interest placed in the left ventricular cavity (~ 300 mm²) and over the myocardial wall (~ 90 mm²). No retrospective image reregistration was necessary, since images were acquired during a breath-hold. Solutions containing different concentrations of gadopentetate dimeglumine (1–75 mM) were imaged with IGEPI and compared with conventional fast gradient-echo images to assess how the presence of an echo train affects the sequence's sensitivity to an MR contrast agent.

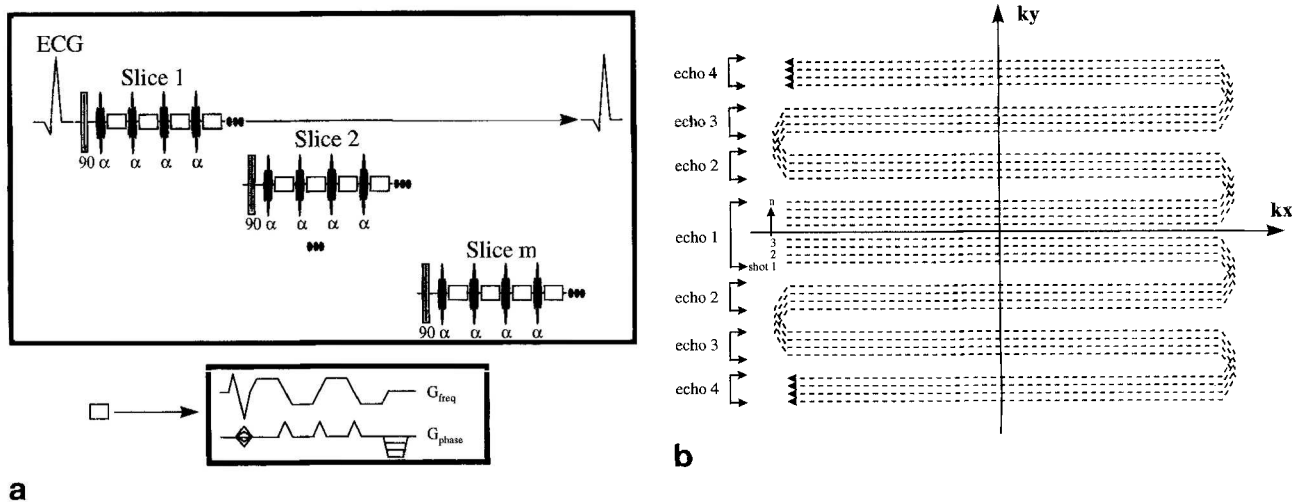


FIG. 1. (a) Schematic for IGEPI with an ETL of 4. Within each R-R interval, slices 1 through m are acquired sequentially. For each slice, a volumetric saturation pulse (90°) is followed by a series of α pulses. For each α pulse, four gradient echoes are acquired covering four lines of k -space. The bottom box shows the frequency- and phase-encoding gradients applied after each α pulse. The phase-encoding gradients and blips were rewound at the end of the echo train. (b) Schematic for k -space trajectory with n shots.

RESULTS

Figure 2a shows eight short-axis slice locations acquired from a normal volunteer. Fig. 2b shows the contrast bolus pass through the right ventricle, left ventricle, and myocardium for a single-slice location. The signal intensity versus time curves for the left ventricular blood pool and a region of interest in the myocardium are shown in Fig. 2c. The regions of interest used for this analysis are shown in Fig. 2d.

Because the cardiac apex is difficult to evaluate on short-axis images due to partial volume effects, the possibility of collecting long-axis as well as short-axis images during the same contrast bolus was assessed. The application of a volume-selective saturation pulse before

each slice allows acquisition of multiple images with overlapping locations without slice-to-slice interference during a single scan. Figure 3 shows four short-axis slices and one long-axis slice acquired with IGEPI from a normal volunteer.

Figure 4 shows how signal intensity varies as a function of gadopentetate dimeglumine concentration using fast gradient echo and IGEPI with an ETL of 4. Both signal intensity curves are normalized to the signal intensity with lowest concentration. Figure 4b shows expanded scale in the concentration range from 1 to 5 mM. Both sequences show an approximately linear relationship between gadopentetate dimeglumine concentration and signal intensity in this range ($R^2 = 0.99$ for both). The decrease in signal intensity that occurs at concentra-

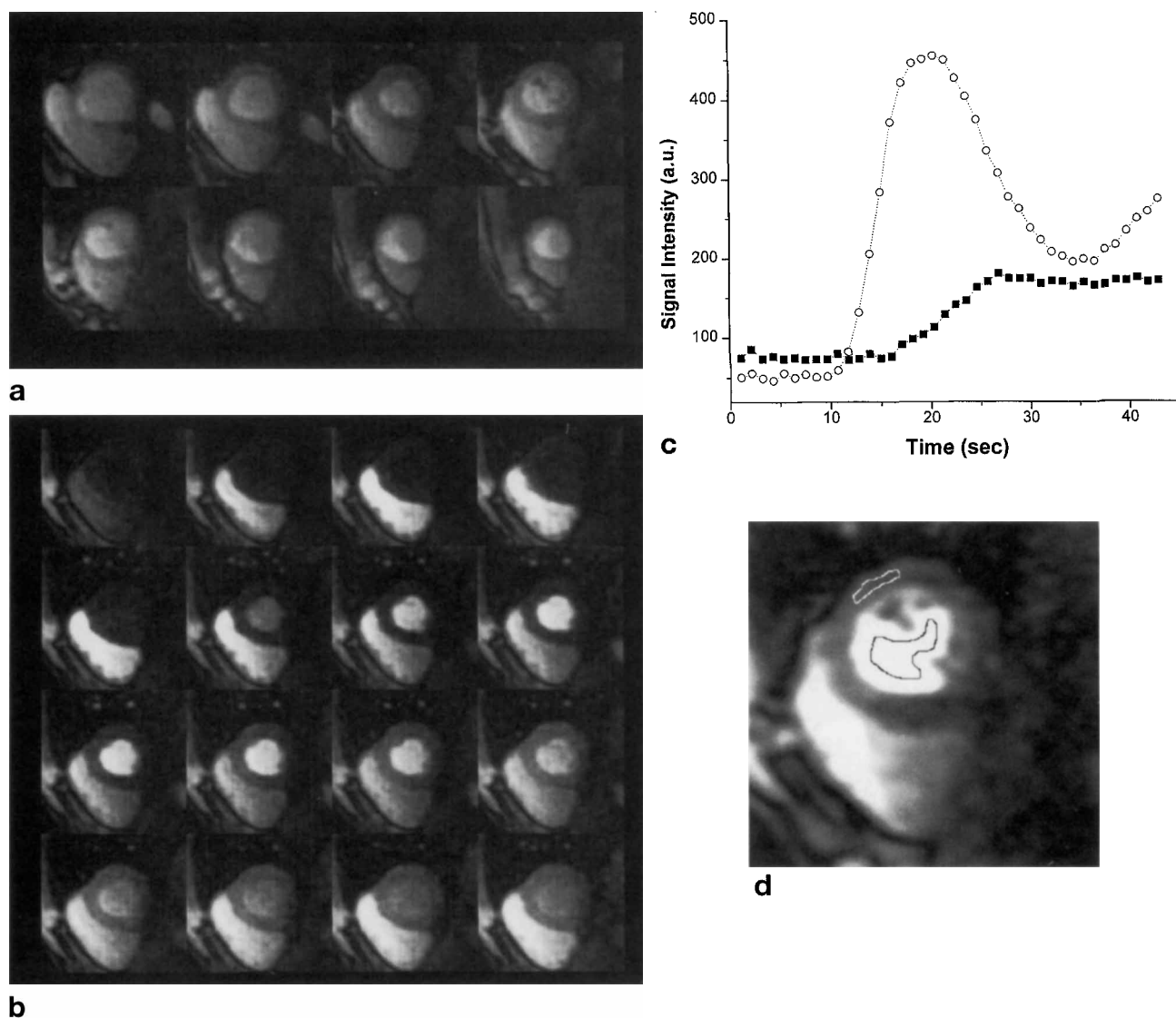


FIG. 2. (a) Eight short-axis slices from a normal volunteer with a heart rate of 56 beats/min. Acquisition parameters: raw data matrix, 128×48 ; FOV, 39×19 cm; TR, 6.6 ms; TE_{eff} , 2 ms; receiver bandwidth, ± 125 KHz; slice thickness, 8 mm; acquisition time per image, 100 ms; 12 shots. Contrast dose = 0.07 mmol/Kg. (b) First-pass time course for a mid-ventricular short-axis slice. For display purposes, images from only every other heart beat are shown. Time increases from left to right, then from top to bottom. The contrast bolus sequentially passes from right ventricle to left ventricle and finally to the myocardium. (c) Signal intensity versus time for the left ventricular blood pool and left ventricular myocardium. (d) Regions of interest for signal intensity analysis.

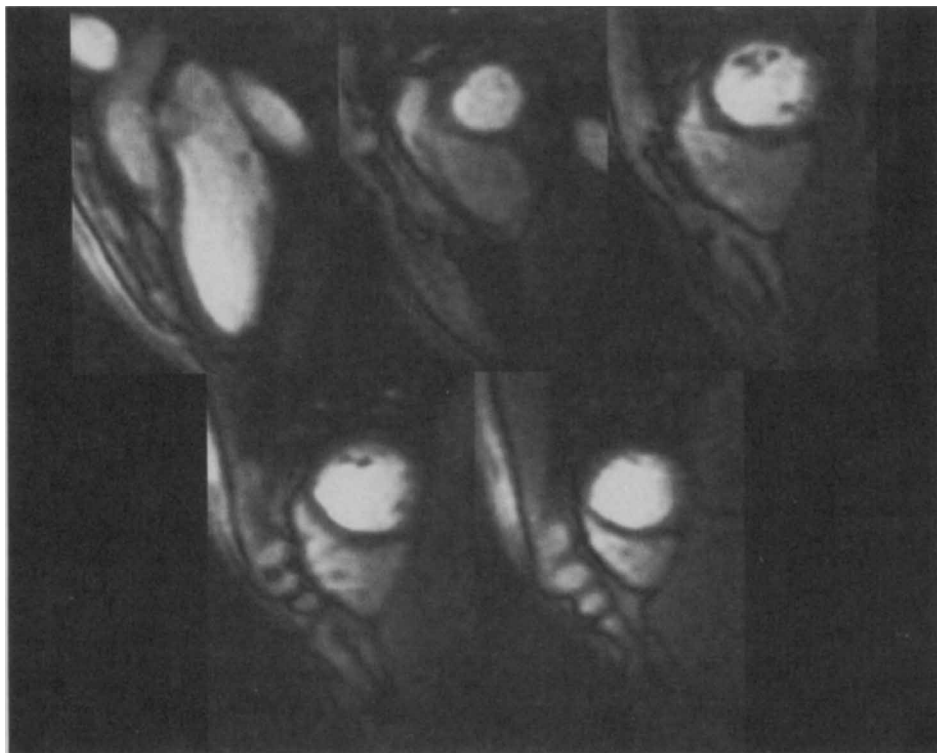
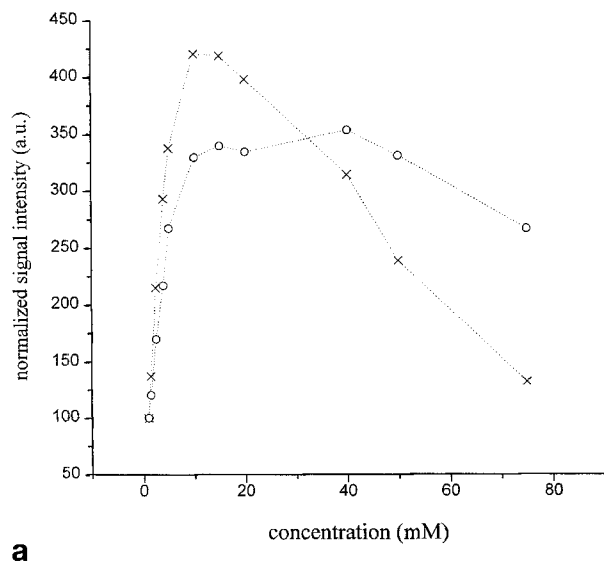


FIG. 3. One long-axis slice and four short-axis slices from a normal volunteer with a heart rate of 67 beats/min. Acquisition parameters: raw data matrix, 128×72 ; FOV, 36×27 cm; TR, 7 ms; TE_{eff} , 2 ms; receiver bandwidth, ± 125 KHz; slice thickness, 8 mm; acquisition time per image, 146 ms; 18 shots. Contrast dose = 0.04 mmol/kg.

tions greater than 20 mM is more pronounced for IGEPI as compared with fast gradient echo, as shown in Fig. 4a. This is due to T_2^* modulation of the echo train.



1993 for cardiac imaging and functional brain imaging. We have modified the original IGEPI sequence for dynamic contrast-enhanced cardiac imaging by adding a

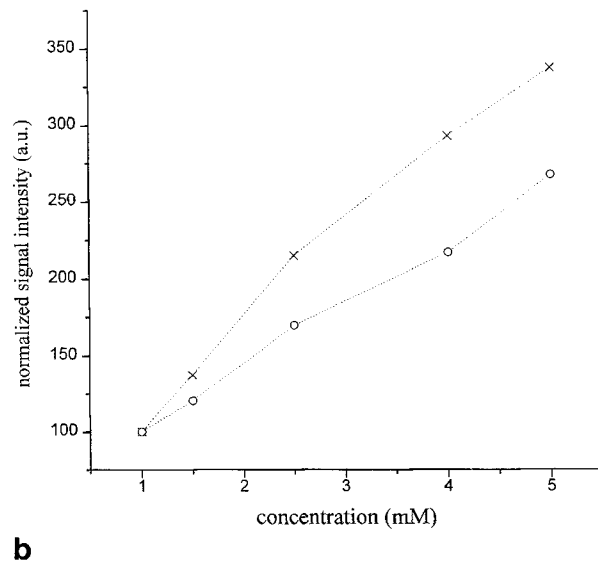


FIG. 4. (a) Signal intensity versus concentration for solutions containing gadopentetate dimeglumine. Signal intensity is normalized to the signal at the lowest concentration. Open circles correspond to measurements made with fast gradient echo. Crosses correspond to measurements made with IGEPI with an ETL of 4. The decrease in signal intensity that occurs at concentrations greater than 20 mM is due to T_2^* relaxation. (b) Expanded scale at low gadopentetate dimeglumine concentrations. Both sequences show an approximately linear relationship between gadopentetate dimeglumine concentration and signal intensity between 1 and 5 mM ($R^2 = 0.99$ for both).

DISCUSSION

We have modified IGEPI to better satisfy the requirements for first-pass contrast-enhanced cardiac imaging. Compared to fast gradient echo, IGEPI provides improved coverage because it has a higher acquisition duty cycle; in addition, compared with single- or dual-shot EPI, it is less sensitive to susceptibility-related artifacts and is compatible with quantitative assessment of perfusion. Because a volume-selective saturation prepulse was applied before each slice, images in different overlapping planes could be acquired without slice-to-slice interference. This coupled with improved speed enabled the acquisition of both short- and long-axis planes during a single scan, which provides the advantage of being able to assess the same region of myocardium on two independent images of different orientation.

IGEPI was implemented previously by McKinnon (22) in

saturation prepulse to null the longitudinal magnetization before the image acquisition and by using a phase encoding order that minimizes the effective echo time. The volumetric saturation prepulse before IGEPI is used to obtain T_1 weighting, insensitivity to arrhythmia (14, 18), and insensitivity to through-plane flow/motion. Gradient moment nulling was not implemented in the original IGEPI sequence (22). However, we have found that this technique when applied along the slice and readout directions is effective in reducing image artifacts caused by flow and motion.

Looking toward the possibility of using IGEPI for quantitative myocardial perfusion measurements, we used solutions containing gadopentetate dimeglumine (1–75 mM) to assess how signal intensity varies as a function of gadopentetate dimeglumine concentration for fast gradient echo and IGEPI with an ETL of 4. We found that the curve describing signal intensity versus gadopentetate dimeglumine concentration for IGEPI is linear over approximately the same range as for fast gradient echo (Fig. 4). Based on this, we expect that IGEPI provides an estimate of the input function, using the ventricle time-intensity curve, similar to that obtainable by fast gradient echo. Single- and dual-shot spin echo EPI do not provide this information (15, 16).

Both EPI and magnetization-prepared fast gradient echo have previously been shown to be susceptible to image artifacts. This occurs for EPI because image data are acquired while the MR signal undergoes T_2^* relaxation and because off-resonance effects accumulate (20, 22, 25). For magnetization-prepared fast gradient echo, this occurs because image data are acquired while the MR signal undergoes T_1 relaxation toward a steady state (26–28). Technical solutions for reducing these artifacts have also been developed previously. The modified IGEPI sequence is susceptible to artifacts related to T_2^* relaxation, off-resonance effects, and T_1 relaxation. To reduce image artifacts for the IGEPI sequence, we implemented and evaluated some of the techniques from EPI and magnetization-prepared fast gradient echo. Specifically, we found that the EPI techniques of echo shifting (20, 22, 29) and using a phase-encoding order designed to cause smooth variations in k -space related to T_2^* decay and off-resonance effects were very important in reducing artifacts. We have also implemented and are currently evaluating techniques associated with the magnetization-prepared fast gradient echo approach to steady state such as RF spoiling (30–32) and variable flip angle excitation (22, 33, 34), which may reduce the magnitude modulation of k -space data due to T_1 relaxation, resulting in an improved point spread function. More generally, signal modulation due to T_1 and T_2^* relaxation and off-resonance effects contribute to a nonideal point spread function. Future work will focus on assessing and improving the point spread function for the modified IGEPI sequence. Finally, in our experience with normal volunteers, we have not found the chemical shift of fat in the phase-encoding direction to be problematic. This is due to the saturation prepulse that also acts as a fat suppression pulse.

In conclusion, by using a relatively short echo train, some of the speed advantages of EPI are achieved without

encountering artifacts related to magnetic susceptibility interfaces seen using single-shot or dual-shot EPI. By acquiring multiple views per RF pulse, speed is improved (number of lines acquired per unit time increased) compared with fast gradient echo without using extremely short TR values and sacrificing SNR. The modified IGEPI technique provides an approach that combines EPI speed and fast gradient-echo image quality and has the potential for assessing myocardial perfusion by MRI with combined spatial resolution, temporal resolution, image quality, and the potential for quantitation that are superior to fast-gradient echo and single- or dual-shot EPI. In addition, short- and long-axis images can be acquired simultaneously, enabling the assessment of the same myocardial region in two different views.

ACKNOWLEDGMENTS

The authors thank Thomas K. F. Foo for help in pulse sequence development.

REFERENCES

1. B. L. Holman, "Heart Disease: A Textbook of Cardiovascular Medicine," Saunders, Philadelphia, 1988.
2. R. C. Marshall, J. H. Tillisch, M. E. Phelps, S. C. Huang, R. Carson, E. Henze, H. R. Schelbert, K. L. Gould, Identification and differentiation of resting myocardial ischemia and infarction in man with positron computed tomography, ^{18}F -labeled fluorodeoxyglucose and N-13 ammonia: detecting and assessing severity of coronary artery disease in humans. *Cardiovasc. Intervent. Radiol.* **13**, 5–13 (1990).
3. S. Sawada, O. Muzik, R. S. B. Beanlands, E. Wolfe, G. D. Hutchins, M. Schwaiger, Interobserver and interstudy variability of myocardial blood flow and flow reserve measurements with nitrogen 13 ammonia-labeled positron emission tomography. *J. Nucl. Cardiol.* **2**, 413–422 (1995).
4. A. Bol, J. A. Melin, J. L. Vanoverschelde, A. Robert, G. R. Heyndrickx, W. Wijns, T. Baudhuin, D. Vogelaers, M. De Pauw, C. Michel, A. Luxen, D. Labar, M. Cogneau, et al., Direct comparison of ^{13}N ammonia and ^{15}O water estimates of perfusion with quantification of regional myocardial blood flow by microspheres. *Circulation* **87**, 512–525 (1993).
5. J. Hartiala, J. Knuuti, Imaging of the heart by MRI and PET. *Ann. Med.* **27**, 35–45 (1995).
6. E. Pauwels, A. de Roos, Nuclear medicine techniques and magnetic resonance imaging in coronary artery disease. *Q. J. Nucl. Med.* **40**, 132–141 (1996).
7. D. J. Atkinson, D. Burstein, R. R. Edelman, First-pass cardiac perfusion: evaluation with ultrafast MR imaging. *Radiology* **174**, 757–762 (1990).
8. A. C. Eichenberger, E. Schuiki, V. D. Kochli, F. W. Amann, G. C. McKinnon, G. K. von Schulthess, Ischemic heart disease: assessment with gadolinium-enhanced ultrafast MR imaging and dipyridamole stress. *J. Magn. Reson. Imaging* **4**, 425–431 (1994).
9. S. Schaefer, R. van Tyen, D. Saloner, Evaluation of myocardial perfusion abnormalities with gadolinium-enhanced snapshot MR imaging in humans: work in progress. *Radiology* **185**, 795–801 (1992).
10. N. Wilke, C. Simm, J. Zhang, J. Ellermann, X. Ya, H. Merkle, G. Path, H. Ludemann, R. J. Bache, K. Ugurbil, Contrast-enhanced first pass myocardial perfusion imaging: correlation between myocardial blood flow in dogs at rest and during hyperemia. *Magn. Reson. Med.* **29**, 485–497 (1993).
11. N. Wilke, K. Kroll, H. Merkle, Y. Wang, Y. Ishibashi, Y. Xu, J. Zhang, M. Jerosch-Herold, A. Muhler, A. E. Stillman, J. B. Bassingthwaighte, R. Bache, K. Ugurbil, Regional myocardial blood volume and flow: first-pass MR imaging with polylysine-Gd-DTPA. *J. Magn. Reson. Imaging* **5**, 227–237 (1995).
12. J. B. Bassingthwaighte, G. R. Raymond, J. I. S. Chan, Principles of tracer kinetics, in "Nuclear Cardiology: State of the Art and Future Directions" (B. L. Zaret, G. A. Beller, Eds.), p. 3, Mosby-Year Book, St. Louis, 1993.

13. W. J. Manning, D. J. Atkinson, W. Grossman, S. Paulin, R. R. Edelman, First-pass nuclear magnetic resonance imaging studies using gadolinium-DTPA in patients with coronary artery disease. *J. Am. Coll. Cardiol.* **18**, 959–965 (1991).
14. N. V. Tsekos, Y. Zhang, H. Merkle, N. Wilke, M. Jerosch-Herold, A. Stillman, K. Ugurbil, Fast anatomical imaging of the heart and assessment of myocardial perfusion with arrhythmia insensitive magnetization preparation. *Magn. Reson. Med.* **34**, 530–536 (1995).
15. J. F. Debatin, G. C. McKinnon, G. K. von Schulthess, Technical note: approach to myocardial perfusion with echo planar imaging. *MAGMA* **4**, 7–11 (1996).
16. R. R. Edelman, W. Li, Contrast-enhanced echo-planar MR imaging of myocardial perfusion: preliminary study in humans. *Radiology* **190**, 771–777 (1994).
17. J. Schwitter, J. F. Debatin, G. K. von Schulthess, G. C. McKinnon, Normal myocardial perfusion assessed with multishot echo-planar imaging. *Magn. Reson. Med.* **37**, 140–147 (1997).
18. N. Wilke, M. Jerosch-Herold, Y. Wang, Y. Huang, B. V. Christensen, A. E. Stillman, K. Ugurbil, K. McDonald, R. F. Wilson, Myocardial perfusion reserve: assessment with multisection, quantitative, first-pass MR imaging. *Radiology* **204**, 373–384 (1997).
19. F. Farzaneh, S. J. Riederer, N. J. Pelc, Analysis of T2 limitations and off-resonance effects on spatial resolution and artifacts in echo-planar imaging. *Magn. Reson. Med.* **14**, 123–139 (1990).
20. Z. H. Cho, C. B. Ahn, J. H. Kim, Y. E. Lee, C. W. Mun, Phase error corrected interlaced echo planar imaging, in "Proc., SMRM, 6th Annual Meeting, New York, 1987," p. 912.
21. F. Farzaneh, S. J. Riederer, J. K. Maier, R. Vavrek, View-interleaved EPI on a commercial scanner, in "Proc., SMRM, 8th Annual Meeting, Amsterdam, 1989," p. 832.
22. G. C. McKinnon, Ultrafast interleaved gradient-echo-planar imaging on a standard scanner. *Magn. Reson. Med.* **30**, 609–616 (1993).
23. S. E. Fischer, S. A. Wickline, C. H. Lorenz, Multiple slice hybrid imaging sequence for myocardial perfusion measurement, in "Proc., ISMRM, 4th Annual Meeting, New York, 1996," p. 682.
24. S. E. Fischer, J. P. Groen, R. E. Henson, C. A. White, M. P. Watkins, S. A. Wickline, C. H. Lorenz, Myocardial perfusion assessment of the entire heart, in "Proc., ISMRM, 5th Annual Meeting, Vancouver, 1997," p. 478.
25. D. A. Feinberg, K. Oshio, Phase errors in multi-shot echo planar imaging. *Magn. Reson. Med.* **32**, 535–539 (1994).
26. A. Haase, R. Matthaei, R. Bartkowski, E. Duhmke, D. Leibfritz, Inversion recovery snapshot FLASH MR imaging. *J. Comput. Assist. Tomogr.* **13**, 1036–1040 (1989).
27. W. Hanicke, K. D. Merboldt, D. Chien, M. L. Gyngell, H. Bruhn, J. Frahm, Signal strength in sub-second FLASH magnetic resonance imaging: the dynamic approach to steady state. *Med. Phys.* **17**, 1004–1010 (1990).
28. R. A. Jones, P. A. Rinck, Approach to equilibrium in snapshot imaging. *Magn. Reson. Imaging* **8**, 797–803 (1990).
29. D. A. Feinberg, K. Oshio, Gradient-echo shifting in fast MRI techniques (GRASE imaging) for correction of field inhomogeneity errors and chemical shift. *J. Magn. Reson.* **97**, 177–183 (1992).
30. A. P. Crawley, M. L. Wood, R. M. Henkelman, Elimination of transverse coherences in FLASH MRI. *Magn. Reson. Med.* **8**, 248–260 (1988).
31. F. H. Epstein, J. P. I. I. I. Mugler, J. R. Brookeman, Spoiling of transverse magnetization in gradient-echo (GRE) imaging during the approach to steady state. *Magn. Reson. Med.* **35**, 237–245 (1996).
32. Y. Zur, M. L. Wood, I. J. Neuringer, Spoiling of transverse magnetization in steady-state sequences. *Magn. Reson. Med.* **21**, 251–263 (1991).
33. M. K. Stehling, Improved signal in "snapshot" FLASH by variable flip angles. *Magn. Reson. Imaging* **10**, 165–167 (1992).
34. J. P. Mugler III, F. H. Epstein, J. R. Brookeman, Shaping the signal response during the approach to steady state in three-dimensional magnetization-prepared rapid gradient-echo imaging using variable flip angles. *Magn. Reson. Med.* **28**, 165–185 (1992).